

# Ageing and Quenching: Influence of Galaxy Environment and Nuclear Activity in Transition Stage

Pius Privatus<sup>1,2,\*</sup> and Umananda Dev Goswami<sup>1,†</sup>

<sup>1</sup>*Department of Physics, Dibrugarh University, Dibrugarh 786004, Assam, India*

<sup>2</sup>*Department of Natural Sciences, Mbeya University of Science and Technology, Iyunga 53119, Mbeya, Tanzania*

This study aims to investigate whether the environment and the nuclear activity of a particular galaxy influence the ageing and quenching at the transition stage of the galaxy evolution using the volume-limited sample constructed from the twelve release of the Sloan Digital Sky Survey. To this end, the galaxies were classified into isolated and non-isolated environments and then each subsample was further classified according to their nuclear activity using the WHAN diagnostic diagram, and ageing diagram to obtain ageing and quenching galaxies. The ageing and quenching galaxies at the transition stage were selected for the rest of the analysis. Using the star formation rate and the  $u-r$  colour-stellar mass diagrams, the study revealed a significant change of 0.03 dex in slope and 0.30 dex in intercept for ageing galaxies and an insignificant change of 0.02 dex in slope and 0.12 dex in intercept of the star formation main sequence between isolated and non-isolated quenching galaxies. Further, a more significant change in the number of ageing galaxies above, within and below the main sequence and the green valley was observed. On the other hand, an insignificant change in the number of quenching galaxies above, within and below the main sequence and the green valley was observed. The study concludes that ageing depends on the environment and the dependence is influenced by the nuclear activity of a particular galaxy while quenching does not depend on the environment and this independence is not influenced by the nuclear activity.

Keywords: Ageing; Quenching; Main sequence; Green valley; Galaxy environment.

## I. INTRODUCTION

The processes of galaxy evolution and the end of star formation within the galaxy remain unsolved issues in astrophysics to date. This is due to the complex nature of the physical processes underlying this field, despite the fact that the relation between the star formation history (SFH) of galaxies and their physical properties such as stellar mass, environment, morphology and chemical composition has been extensively studied during the last few decades [1–3]. The relations between the physical properties of galaxies have been proven to be bimodal distributions [3, 4]. This led to the division of the galaxies into the galaxies within, above and below the main sequence (MS), where on the MS are normal star forming galaxies, above are the starburst galaxies which undergo excess star formation and below the MS are passive galaxies with little star formation [5–13]. On the other hand, galaxies have also been divided into star forming galaxies with abundant gas reservoirs and passive galaxies that correspond to poor gas and early-type systems [14, 15]. The star forming was observed to be in the blue cloud (BC), while the retired galaxies were in red sequence (RS). The galaxies in intermediate were defined to be in the green valley (GV) in colour against stellar mass diagrams [16–18].

In recent years different internal (secular) and external (environmental) processes have been proposed as the main reason for the transition from the BC to the RS characterised by the decrease in star formation rate (SFR) referred to as quenching. For the internal processes the galaxy may quench due to internally triggered quenching mechanisms such as negative feedback from Active Galactic Nuclei (AGN), supernovae winds or the stabilisation of the gas against fragmentation [19, 20]. On the other hand, external processes triggered quenching may be due to environmentally driven processes such as ram pressure stripping able to remove the gas reservoir, strangulation or starvation (leading to the suppression of gas infall or galaxy interactions) [21, 22]. Although these processes are observed to slow down the rate of star formation but also enhance the star formation in a short time scale [23].

Quenching has been categorised into fast and slow quenching depending on the duration of time spent to cross an arbitrary boundary in the stellar mass ( $M_*$ ) versus specific star formation rate ( $SSFR = SFR/M_*$ ) plane and colour-magnitude diagram [24–26]. The fast quenching involves the termination of SFR in a short time scale that is less than 1 Gyr and slow quenching involves the termination of SFR with a time scale comparable to the age of the universe. Usually, the term quenching has been defined as a process able to terminate the star formation process in a short time scale in reference to the age of the universe while the term ageing denotes the continuous evolution of a galaxy through a secular process. Ageing is different but difficult to distinguish from the slow quenching [27, 28]. In this work, we will continue to use quenching and ageing as defined in Refs. [27, 28].

\* Email: [privatuspius08@gmail.com](mailto:privatuspius08@gmail.com)

† Email: [umananda@dibru.ac.in](mailto:umananda@dibru.ac.in)

Ref. [29], studied the radial profiles in  $H\alpha$  equivalent width and SSFR derived from spatially resolved MaNGA survey as detailed in Ref. [30], to gain insight into the physical mechanisms that suppress the star formation, and observed that the responsible quenching mechanism appears to affect the entire galaxy. Ref. [31] obtained that morphology and environment have a combined role in slowing down the star formation activities in galaxies. Furthermore, they observed that a long-timescale environmental effect appears at low redshift. Ref. [32] suggested that the decrease of SFR is mainly due to internal and linked with bulge growth. However, the existence of the relation between morphology and density may provide a different turn in the relation of SFR, stellar mass and the environment where a particular galaxy resides. The study by Ref. [33], presenting the analysis of star formation and quenching in the SDSS MaNGA survey as detailed in Ref. [30], utilising over 5 million spaxels from  $\sim 3500$  local galaxies observed that the sudden decrease of SFR affect the whole galaxy but star formation occurs in a small localised scale within the galaxy. On the other hand Ref. [33] observed that quenching is global while star formation is governed by local processes within each pixel. All these studies aim to discern the mechanism or combination of mechanisms that lead to the quenching of star formation processes in galaxies, thereby influencing their evolution.

In a simplified representation, the process guiding these transformations can be broadly categorised as ‘internal’ and ‘external’. Rather than being driven by stochastic events like massive mergers and starbursts, Ref. [6] demonstrated that the normalisation declines dramatically but steadily as a function of redshift, possibly on mass-dependent time scales. Keeping in mind that the more precise relation of redshift on evolution is often expressed as  $\propto (1+z)^\gamma$ , with  $\gamma$  which range from 1.9 to 3.7 [34–36]. Ref. [37], using the model of galaxy formation, observed the AGN feedback to be the primary mechanism affecting quenching. Although this may affect the massive galaxies ( $10^{11} M_\odot$ ), there is a lack of observed feedback effects for the majority of the star forming galaxies [38]. However, Ref. [39] using a basic model for disk evolution, demonstrated that the evolution of galaxies away from the main sequence can be attributed to the depletion of gas due to star formation after a cut-off of gas inflow. This model was based on the observed dependence of star formation on gas content in local galaxies and assuming simple histories of cold gas inflow. Again Ref. [39] using the MS as the tracer of the factors responsible for quenching further obtained that galaxies classified as MS, quiescent, or passive exhibit varying fractions on mass and environment. The MS fractions decrease with increasing mass and density, while the quiescent and passive fractions rise. Due to this uncertainty, the ongoing debate revolves around the extent to which each of these scenarios influences the shape of the relationship.

By examining the physical characteristics of MaNGA as detailed in Ref. [30] and SAMI as detailed in Refs. [40, 41], Ref. [28] found that the ageing population is made up of a heterogeneous mixture of galaxies, primarily late-type systems, with a range of physical features. Authors pointed out that the retired were formerly ageing or quenched systems and are either in low or denser environments. The study shows that distinguishing between old (retired) and recently quenched galaxies are important to constrain the mechanisms driving galaxy evolution. The study left two very important questions regarding the role of environment: did the galaxies simply evolve on shorter time scales over cosmic history because they arise from a higher over-density peak in the primordial universe (nature) or whether the galaxies tend to be compact due to an externally induced process (nurture)?

As the follow-up of the work by Ref. [28], this study aims to investigate whether the environment influences ageing and quenching, and how their relationships with the environment are affected by nuclear activity. This study uses the friends-of-friend method from Ref. [42], to assign ageing and quenching galaxies in a transition stage into systems of isolated (with no neighbour) and non-isolated (with at least one neighbour) environment and then to compare their equations of the main sequence, the colour obtained from  $u$ - and  $r$ -band luminosities ( $u-r$  colour) and stellar mass diagrams.

Our paper is organized as follows. In the next section, we explain the source of data and the method of getting samples. In Section III we explain the methodology used in this study. The Section IV is dedicated to presenting the results. In Section V the results are discussed. Section VI presents the summary and conclusion. Cosmological constants used in this work are adopted from Ref. [43], wherein the dark energy density parameter  $\Omega_\Lambda = 0.692$ , Hubble constant  $H_0 = 67.8 \text{ km s}^{-1} \text{ Mpc}^{-1}$  and the matter density parameter  $\Omega_m = 0.308$  are recorded.

## II. DATA

### A. The SDSS main sample

In this research work the catalogue data extracted from the flux-limited sample of twelve releases of Sloan Digital Sky Survey (SDSS DR12) as detailed in Ref. [44, 45] are used. The main galaxy sample was selected from the main contiguous area of the survey based on the methods outlined in Ref. [42]. Galaxy data were downloaded from the SDSS Catalogue Archive Server (CAS). The objects with the spectroscopic class GALAXY or QSO as detailed in Ref. [45], were selected as suggested by the SDSS team. We then filtered out galaxies with the galactic-extinction-correction based on Ref. [46] where Petrosian  $r$ -band magnitude fainter than 17.77 are rejected keeping in mind that the SDSS is incomplete at fainter magnitudes [47]. After correcting the redshift for the motion with respect to the cosmic microwave background (CMB), using the simplified formula  $z_{\text{CMB}} = z_{\text{obs}} - v_p/c$ , where  $v_p$  is a velocity of motion along the line of sight relative to the CMB, the upper distance limit at  $z = 0.2$  was set. The final data set contains 584449 galaxies.

## B. The volume-limited samples

As already stated the SDSS main data are flux-limited, one of the disadvantages of using the flux-limited sample is that only the luminous objects have a chance to be observed at large distances. Due to this main reason, the volume-limited samples are desired. Hence we constructed a volume-limited sample for uniformity. Due to the peculiar velocities of galaxies in groups, the measured redshift (recession velocity) does not give an accurate distance to a galaxy located in a group or cluster, the apparent magnitude was transformed into absolute magnitude using the relation:

$$M_r = m_r - 25 - 5 \log_{10}(d_L) - K, \quad (1)$$

where  $d_L$  is the luminosity distance,  $M_r$  and  $m_r$  are r-band absolute and apparent magnitudes respectively, and  $K$  is the k+e-correction. The k-corrections were calculated with the KCORRECT (*v4.2*) algorithm [48]. The evolution corrections were estimated using the luminosity evolution model of  $K_e = c * z$ , where  $z = -1.62$  for the r-filter [49]. The magnitudes corresponding to the rest frame (at the redshift  $z = 0$ ) and evolution correction were estimated similarly by assuming a distance-independent luminosity function [50, 51]. According to Ref. [52], the Schechter function's [53] typical magnitude  $M_r^*$  is around  $-20.5$  mag. The physical properties of galaxies have been shown to undergo an abrupt transition at the typical magnitude  $M_r^*$ . The variation in the clustering amplitude of galaxies with the absolute magnitude or the galaxy luminosity's environmental dependency is relatively weak for galaxies fainter than  $M_r^*$ , but rather strong for those brighter [54]. We have constructed the volume-limited samples above the characteristic magnitude  $M_r^*$  by calculating the effective maximum distance using the relation as given by

$$d_{\max} = 10^{(m_{r\lim} - M_{r\min} + 5)/5} \times 10^{-6} (\text{Mpc}), \quad (2)$$

where  $m_{r\lim} = 17.17$  mag,  $M_{r\min} = -20.5$  mag. Using the  $d_{\max}$  values and the luminosity restrictions we constructed the volume-limited main galaxy sample containing 136274 galaxies within  $-22.5 \leq M_r \leq -20.5$  (mag).

## III. METHODOLOGY

### A. Isolated and non-isolated environments

Using the volume-limited sample defined in the previous section we assigned the galaxies into isolated and non-isolated subsamples, compiled using the friend-of-friend (FoF) method with a variable linking length. The essence of this approach lies in the division of the sample into distinct systems through an objective and automated process. This involves creating spheres with a linking length ( $R$ ) around each sample point (galaxies). To adjust the linking length based on distance, the procedures outlined in Ref. [42] were applied. The relationship between the linking length and the redshift is represented by an arctangent law as given by

$$R_{LL}(z) = R_{LL,0} \left[ 1 + a \arctan \left( \frac{z}{z_*} \right) \right], \quad (3)$$

where  $R_{LL}(z)$  is the linking length used to create a sphere at a specific redshift,  $R_{LL,0}$  is the linking length at  $z = 0$ ,  $a$  and  $z_*$  are free parameters. The values of  $R_{LL,0} = 0.34$  Mpc,  $a = 1.4$  and  $z_* = 0.09$  are obtained by fitting Eq. (3) to the linking length scaling relation. If there are other galaxies within the sphere, they are considered as the parts of the same system and referred to as "friends". Subsequently, additional spheres are drawn around these newly identified neighbours, and the process continues with the principle that "any friend of my friend is my friend". This iterative procedure persists until no new neighbours or "friends" can be added. At that point, the process concludes, and a system is defined. The galaxies in the system with no neighbour ( $N_{gal} = 1$ ) are isolated, while the galaxies with more than one neighbour ( $N_{gal} \geq 2$ ) are non-isolated. Consequently, each system comprises an isolated galaxy or a non-isolated galaxy that shares at least one neighbour within a distance not exceeding  $R$ . A total of 58032 (42.59%) isolated and 78233 (57.41%) non-isolated galaxies were obtained.

### B. Galaxy properties

The stellar masses used in this study were obtained from the MPA-JHU team and calculated from the Bayesian approach as detailed in Ref. [1]. Stellar mass calculation within the SDSS spectroscopic fiber aperture relies on the fiber magnitudes, whereas the total stellar mass is determined using the model magnitudes.

The MPA-JHU total SFR used in this study was derived from the MPA-JHU database and estimated using the methods of Refs. [2, 4] with adjustments made for non-star forming galaxies. The MPA-JHU team uses the  $H\alpha$  calibration outlined in Ref. [55] to determine the SFR for galaxies classed as star forming. In contrast to the approach taken by Ref. [4], the MPA-JHU team

applied aperture corrections for SFR by fitting the photometric data from the outer regions of the galaxies. Specifically, for SFR computation, Ref. [4] outlined the calculation within the galaxy fiber aperture. It is important to keep in mind that the region beyond the fiber SFR is estimated using the methods of Ref. [56]. Furthermore, for the case of AGN and weak emission line galaxies, SFR was determined using photometry. Keeping in mind that in the case of non-star forming galaxies, the ionisation originates from other sources, such as rejuvenation in the outer regions, post-AGB stars, or ionisation from AGN. As such, the SFR based on  $H\alpha$  for non-star forming galaxies need to be regarded as a maximum value [57].

### C. Galaxy classification

Intending to study where nuclear activity affects the dependence of ageing and quenching on environment, we classified the galaxies based on nuclear activity using the  $W_{H\alpha}$  versus  $[\text{NII}]/H\alpha$  (WHAN) diagram as detailed in Ref. [58], where  $W_{H\alpha}$  is the  $H\alpha$  equivalent width, and  $[\text{NII}]/H\alpha$  is the ratio of the  $[\text{NII}]$  emission line to the  $H\alpha$  line. From this diagram we can have following four inequalities [58]:

$$\log\left(\frac{[\text{NII}]}{H\alpha}\right) < -0.4 \quad \text{and} \quad W_{H\alpha} > 3 \text{ \AA}, \quad (4)$$

$$\log\left(\frac{[\text{NII}]}{H\alpha}\right) > -0.4 \quad \text{and} \quad W_{H\alpha} > 6 \text{ \AA}, \quad (5)$$

$$\log\left(\frac{[\text{NII}]}{H\alpha}\right) > -0.4 \quad \text{and} \quad 3 \text{ \AA} < W_{H\alpha} < 6 \text{ \AA}, \quad (6)$$

$$W_{H\alpha} < 3 \text{ \AA}. \quad (7)$$

These inequalities (4), (5), (6), and (7) represent the pure star-forming (SF) galaxies, strong AGN, weak AGN and retired galaxies (RGs) respectively [58]. The use of the WHAN diagram is based on the fact that the usual traditional diagnostic diagrams detailed in Refs. [11, 59–61], may introduce bias since it is well-known that shock ionisation and AGNs could cover almost any region between the right-low end of the loci usually assigned to SF regions, up to the top-right end of the diagram. On the other hand low-ionisation nuclear emission-line region (LINER) may contain possible multiple ionising sources [58, 62–64]. The distributions of galaxies are shown in Fig. 1 wherein the SF galaxies are shown by blue colour, strong AGN by red colour, weak AGN by green colour and retired galaxies by cyan colour. The following numbers was obtained for isolated galaxies: 30261 ( $\sim 52\%$ ) SF galaxies; 9582 ( $\sim 17\%$ ) strong AGN; 3604 ( $\sim 6\%$ ) weak AGN and 14585 ( $\sim 25\%$ ) retired, while for the non-isolated sample: 31137 ( $\sim 40\%$ ) SF galaxies; 10921 ( $\sim 14\%$ ) strong AGN; 5320 ( $\sim 7\%$ ) weak AGN and 30855 ( $\sim 39\%$ ) retired.

We classified the galaxies into ageing and quenching systems using the ageing diagrams (ADs) as detailed in Ref. [27, 28], given by Eqs. (8) (ageing line) and (9) (quenching line) respectively. The galaxies located above ageing and quenching lines are classified as ageing galaxies (AGs) while the galaxies below ageing and quenching line are quenching galaxies (QGs). The galaxies below the quenching line and above the ageing line are retired while the ones above the quenching line and below the ageing line are undetermined. The ADs are shown in Fig. 2, whereby for isolated a total number of 41886 ( $\sim 72\%$ ), 447 ( $\sim 1\%$ ), 14869 ( $\sim 26\%$ ), and 836 ( $\sim 1\%$ ) were obtained respectively for AGs, QGs, retired and undetermined galaxies, while for non-isolated a total number of 46862 ( $\sim 58\%$ ), 876 ( $\sim 1\%$ ), 31066 ( $\sim 40\%$ ), and 1001 ( $\sim 1\%$ ) were obtained for AGs, QGs, retired and undetermined galaxies. It is very important to keep in mind that in retired galaxies originate from the fast process (quenching) and the slow process (ageing), there is a transition stage given from the colour obtained from  $g$ - and  $r$ -band luminosities ( $u-r$  colour) by  $0.5 < (g-r) < 0.7$  [27]. Since our target is to investigate if the environment is one of the factors for the transition of ageing and quenched galaxies, it is very important to investigate these galaxies in the transition stage. A total of 16929 and 16523 isolated and non-isolated ageing galaxies in transition (AGT) was obtained while a total of 133 and 286 isolated and non-isolated quenched galaxies in the transition stage (QGT) were obtained. We will use the AGT and QGT samples in the next sections unless otherwise stated.

$$\text{Ageing: } \text{EW}(H\alpha)/\text{\AA} = 250.0 \cdot 10^{-1.2 \cdot D_n(4000) - 4.3}, \quad (8)$$

$$\text{Quenched: } \text{EW}(H\alpha)/\text{\AA} = -12.0 \cdot 10^{-0.5 \cdot D_n(4000) + 1.8}. \quad (9)$$

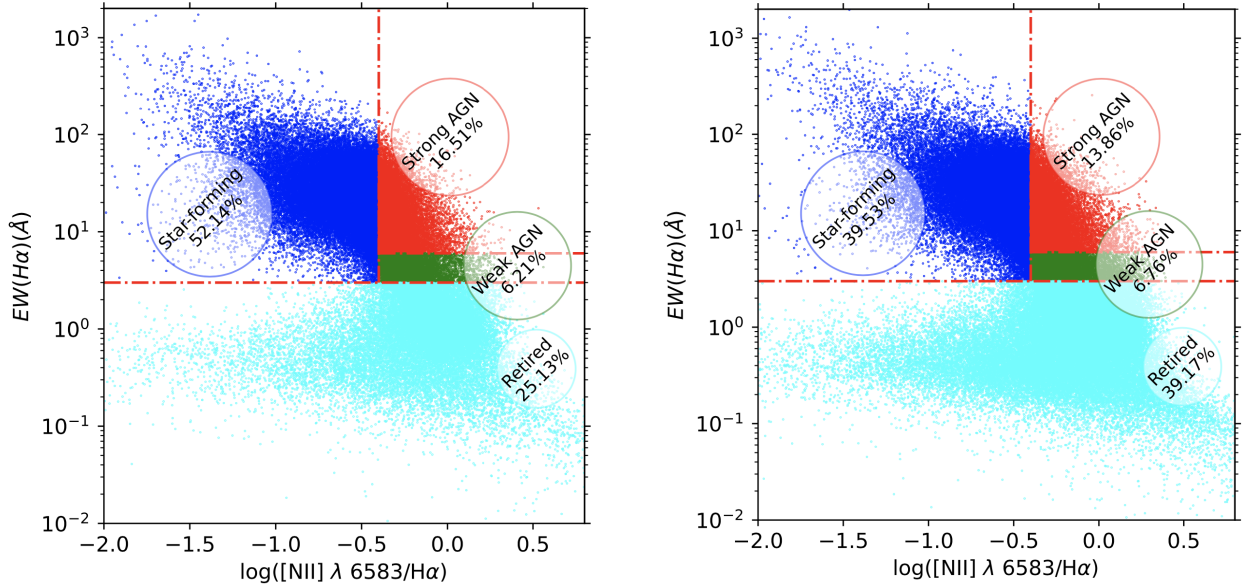


FIG. 1. The WHAN diagrams for the volume-limited main galaxy sample for isolated (left panel) and non-isolated (right panel) cases.

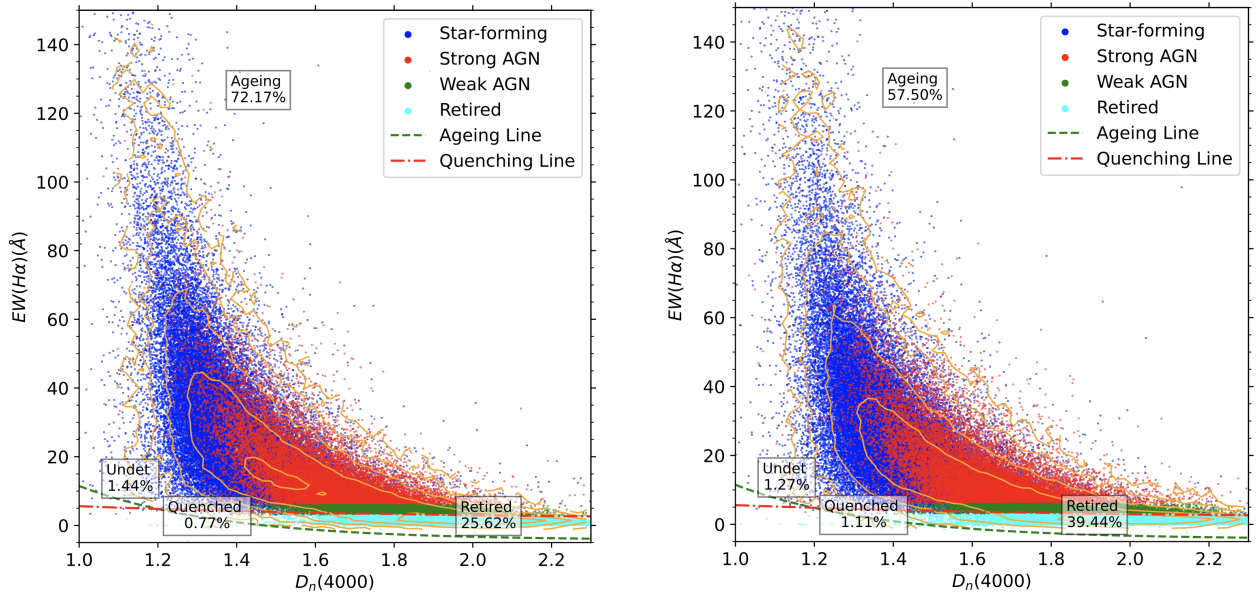


FIG. 2. Ageing diagrams (ADs) for the volume-limited main galaxy sample for isolated (left panel) and non-isolated (right panel) cases.

## IV. RESULTS

### A. Ageing

The equations of the main sequence for SF galaxies show a tight relationship between the  $\log(\text{SFR})$  and  $\log(M_*)$ , and the relation has been studied in a number of works [5–13]. The relationship serves as the tracer on how the stars are formed in relation to the stellar mass within a galaxy. Aiming at studying how the environment affects the SFR relative to the  $M_*$  for the ageing and quenching galaxies, and how the relations are affected by the nuclear activity, we generate the equation of the best-fitted line used to understand the behaviour of SFR relative to  $M_*$  for all galaxies residing in isolated and non-isolated environments. Fig. 3 shows the distributions of SFR with respect to  $M_*$  of the SF, strong AGN, and weak AGN galaxies for isolated and non-isolated cases along with the corresponding best-fitted MS line of the SF galaxies. The width of the MS of

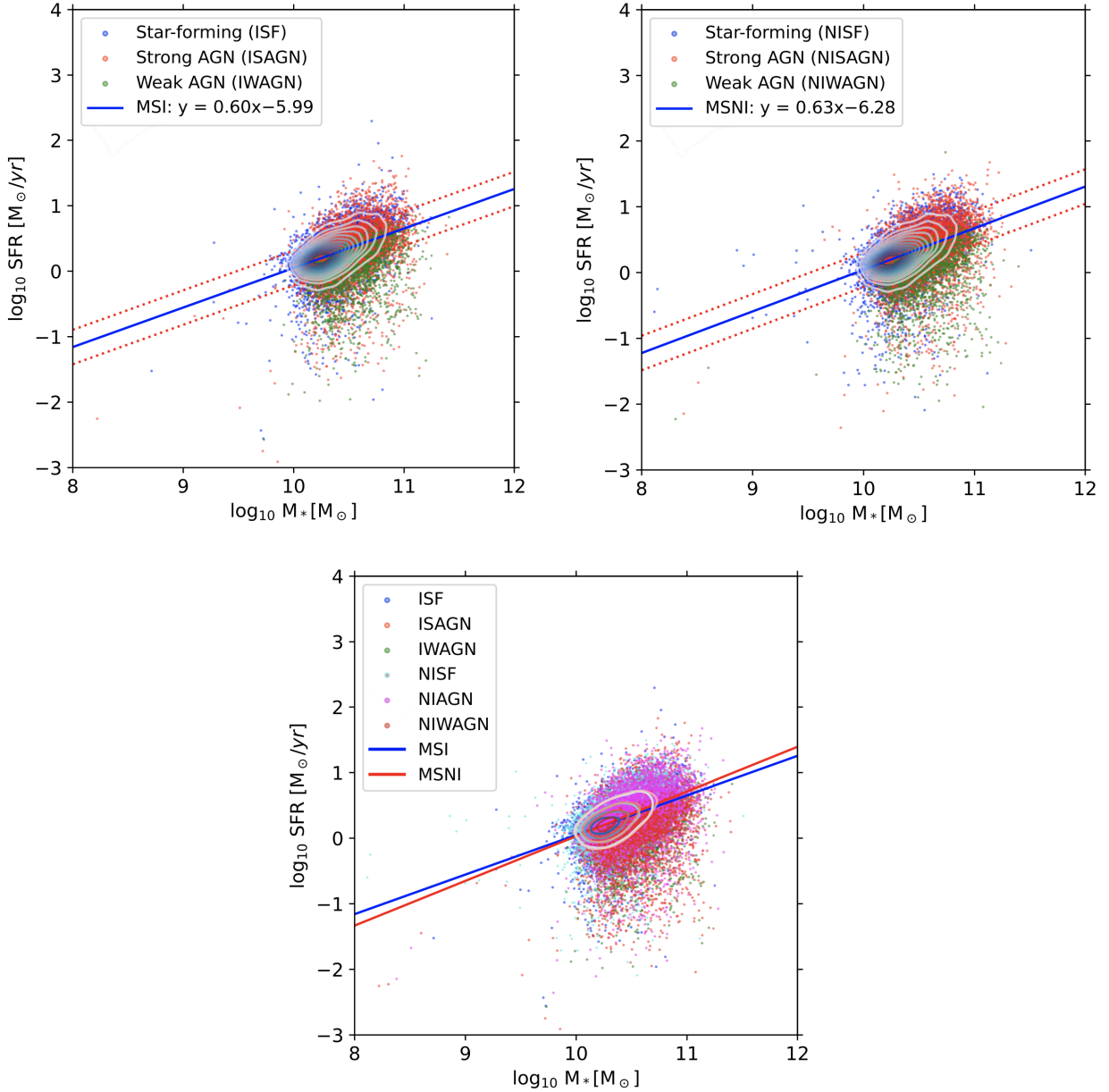


FIG. 3. Star formation main sequence for ageing galaxies: isolated sample (top left panel), non-isolated sample (top right panel), isolated and non-isolated on the same plot (bottom panel).

$\sim \pm 0.3$  dex (red dashed lines) in the plots of this figure is selected based on the dispersion of the observed MS. Table I indicates the percentage change between isolated and non-isolated galaxies above MS, within MS and below MS for SF (columns 2 and 3), Strong AGN (columns 4 and 5), Weak AGN (columns 6 and 7) galaxies, respectively.

By performing the regression analysis for our samples, the general equations of the best-fitted line for the isolated and non-isolated galaxies are respectively given by

$$\log_{10}(\text{SFR}) = 0.60 \pm 0.01 \log_{10}(M_{\star}) - 5.99 \pm 0.14, \quad (10)$$

$$\log_{10}(\text{SFR}) = 0.63 \pm 0.01 \log_{10}(M_{\star}) - 6.28 \pm 0.14, \quad (11)$$

where the associated errors are standard deviations in the slope and intercept.

Galaxies can be categorised further into two groups: those actively forming stars, appearing blue, and those lacking significant star formation, appearing red. The galaxies initially fall into the blue sub-category and then they change gradually to red [14, 15]. It is clear to say that evolution from one category to another must involve processes that quench their rate of forming new stars

TABLE I. Number of galaxies within (MS), above (Above MS), and below (Below MS) the star-forming main sequence for the isolated (iso) and non-isolated (nis) environments for the ageing transition (AGT) volume-limited sample.

Position (1)	Star-forming (%)		Strong AGN (%)		Weak AGN (%)	
	iso (2)	nis (3)	iso (4)	nis (5)	iso (6)	nis (7)
MS	6525(78.04)	6242(78.53)	4709(67.68)	4754(67.75)	610(37.89)	577(37.06)
Above MS	958(11.46)	886(11.15)	782(11.24)	825(11.76)	1(0.06)	1(0.06)
Below MS	878(10.50)	821(10.33)	1467(21.08)	1438(20.49)	999(62.05)	979(62.88)
Total	8361(100)	7949(100)	6958(100)	7017(100)	1610(100)	1557(100)

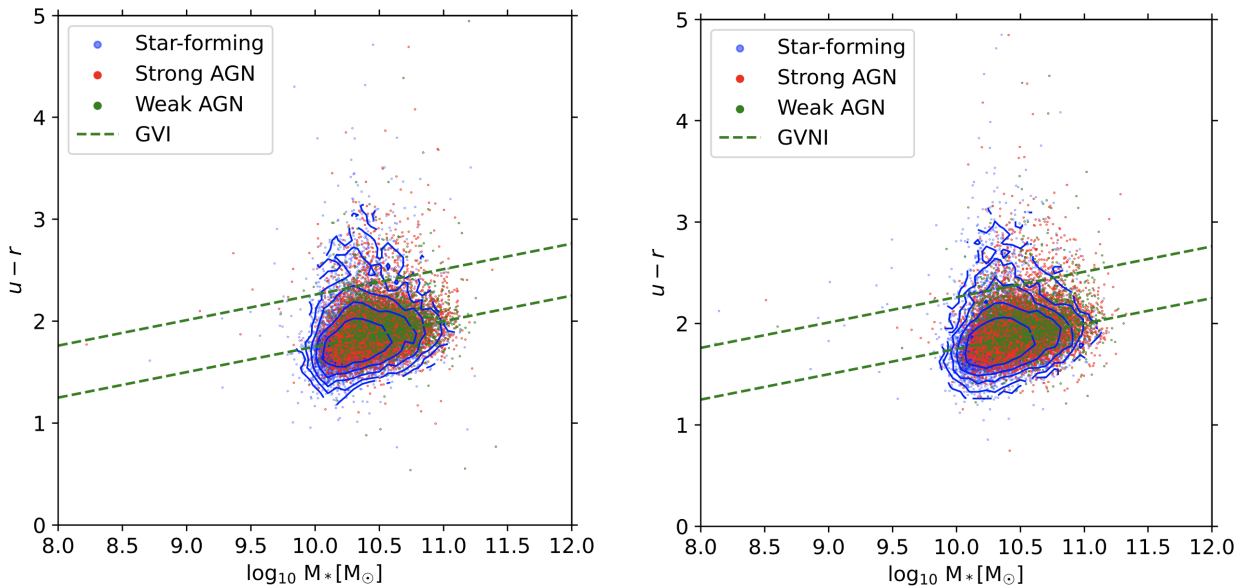


FIG. 4. Ageing galaxies'  $u - r$  colour against stellar mass diagrams for isolated (left panel) and non-isolated (right panel) samples.

from the blue cloud passing the intermediate stage (green valley) to the red sequence [16, 17]. The factors for this transformation may be due to internal mechanisms like negative feedback from the AGNs and the galaxy environment. To study the effect of the environment on colour, Table II shows the number of galaxies with respect to the Green Valley (GV) for ageing galaxies. The position of galaxies on the colour against the stellar mass diagram is shown in Fig 4 for the SF, strong AGN, and weak AGN galaxies respectively. The width of the GV is derived following the criteria from Ref. [18], which is obtained from equations as given by

$$u - r = -0.24 + 0.25 \times M_*, \quad (12)$$

$$u - r = -0.75 + 0.25 \times M_*. \quad (13)$$

Here  $u$  and  $r$  magnitudes were derived from the SDSS database with extinction corrected. Table II indicates the positioning of galaxies with respect to the GV with its percentage for isolated and non-isolated galaxies for the ageing sample above GV, within GV and below GV for SF (columns 2 and 3), strong AGN (columns 4 and 5), weak AGN (columns 6 and 7) galaxies, respectively.

## B. Quenching

As we have done in the previous subsection above, we do the same for the quenching galaxies. Fig. 5, shows the distributions of SFR with respect to  $M_*$  of the SF, strong AGN, and weak AGN galaxies for the isolated and non-isolated cases along with the corresponding best-fitted MS line of the SF for quenching galaxies. By performing regression analysis for our samples, the

TABLE II. Number of galaxies within the green valley (GV), above the green valley (Above GV) and below the green valley (Below GV) for isolated (iso) and non-isolated (nis) galaxies for the ageing sample.

Position (1)	Star-forming (%)		Strong AGN (%)		Weak AGN (%)	
	iso (2)	nis (3)	iso (4)	nis (5)	iso (6)	nis (7)
GV	3334(39.88)	3428(43.12)	3674(52.80)	3800(54.15)	920(57.14)	931(59.79)
Above GV	386(4.62)	424(5.33)	319(4.58)	340(4.85)	90(5.59)	96(6.17)
Below GV	4641(55.51)	4097(51.54)	2965(42.61)	2877(41.00)	600(37.27)	530(34.04)
Total	8361(100)	7949(100)	6958(100)	7017(100)	1610(100)	1557(100)

general equations of the best-fitted line for the isolated and non-isolated galaxies are respectively given by

$$\log_{10}(\text{SFR}) = 0.79 \pm 0.06 \log_{10}(M_{\star}) - 8.38 \pm 0.52, \quad (14)$$

$$\log_{10}(\text{SFR}) = 0.81 \pm 0.04 \log_{10}(M_{\star}) - 8.57 \pm 0.34, \quad (15)$$

where the associated errors are standard deviations in the slope and intercept. Table III indicates the number of galaxies with respect to the MS along with the percentage for the isolated and non-isolated galaxies above MS, within MS and below MS for SF (columns 2 and 3), strong AGN (columns 4 and 5), weak AGN (columns 6 and 7) galaxies, respectively.

TABLE III. Number of galaxies within (MS), above (Above MS), and below (Below MS) the star-forming main sequence for isolated (iso) and non-isolated (nis) environments for the quenching transition (QGT) volume-limited sample.

Position (1)	Star-forming (%)		Strong AGN (%)		Weak AGN (%)	
	iso (2)	nis (3)	iso (4)	nis (5)	iso (6)	nis (7)
MS	78(82.98)	158(76.33)	17(77.27)	25(69.44)	16(94.12%)	32(74.42)
Above MS	4(4.26)	23(11.11)	2(9.09)	7(19.44)	0(0)	1(2.33)
Below MS	12(12.77)	26(12.56)	3(13.64)	4(11.11)	1(5.88%)	10(23.26)
Total	94(100)	207(100)	22(100)	36(100)	17(100)	43(100)

The position of galaxies on the colour against the stellar mass diagram is shown in Fig. 6 for the SF, strong AGN, and weak AGN galaxies respectively. The width of the GV is given by Eqs. (12) and (13). Table IV indicates the positioning of galaxies with respect to the GV with its percentage for isolated and non-isolated galaxies for the quenching sample above GV, within GV and below GV for SF (columns 2 and 3), strong AGN (columns 4 and 5), weak AGN (columns 6 and 7) galaxies, respectively.

Table V indicates the Chi-square P-values between isolated and non-isolated galaxies above MS, within MS and below MS

TABLE IV. Number of galaxies within the green valley (GV), above the green valley (Above GV) and below the green valley (Below GV) for isolated (iso) and non-isolated (nis) galaxies in the quenching sample.

Position (1)	Star-forming (%)		Strong AGN (%)		Weak AGN (%)	
	iso (2)	nis (3)	iso (4)	nis (5)	iso (6)	nis (7)
GV	42(44.68)	95(45.89)	13(59.09)	24(66.67)	12(70.59%)	25(58.14)
Above GV	36(38.30)	95(45.89)	2(9.09)	8(22.22)	4(23.53%)	14(32.56)
Below GV	16(17.02)	17(8.21)	7(31.82)	4(11.11)	1(5.88%)	4(9.30)
Total	94(100)	207(100)	22(100)	36(100)	17(100)	43(100)

for SF (column 2), strong AGN (column 3), weak AGN (column 4) ageing galaxies, respectively and SF (column 5), strong AGN (column 6), weak AGN (column 7) quenching galaxies, respectively. Table VI indicates the Chi-square P-values between isolated and non-isolated galaxies above GV, within GV and below GV for SF (column 2), strong AGN (column 3), weak AGN



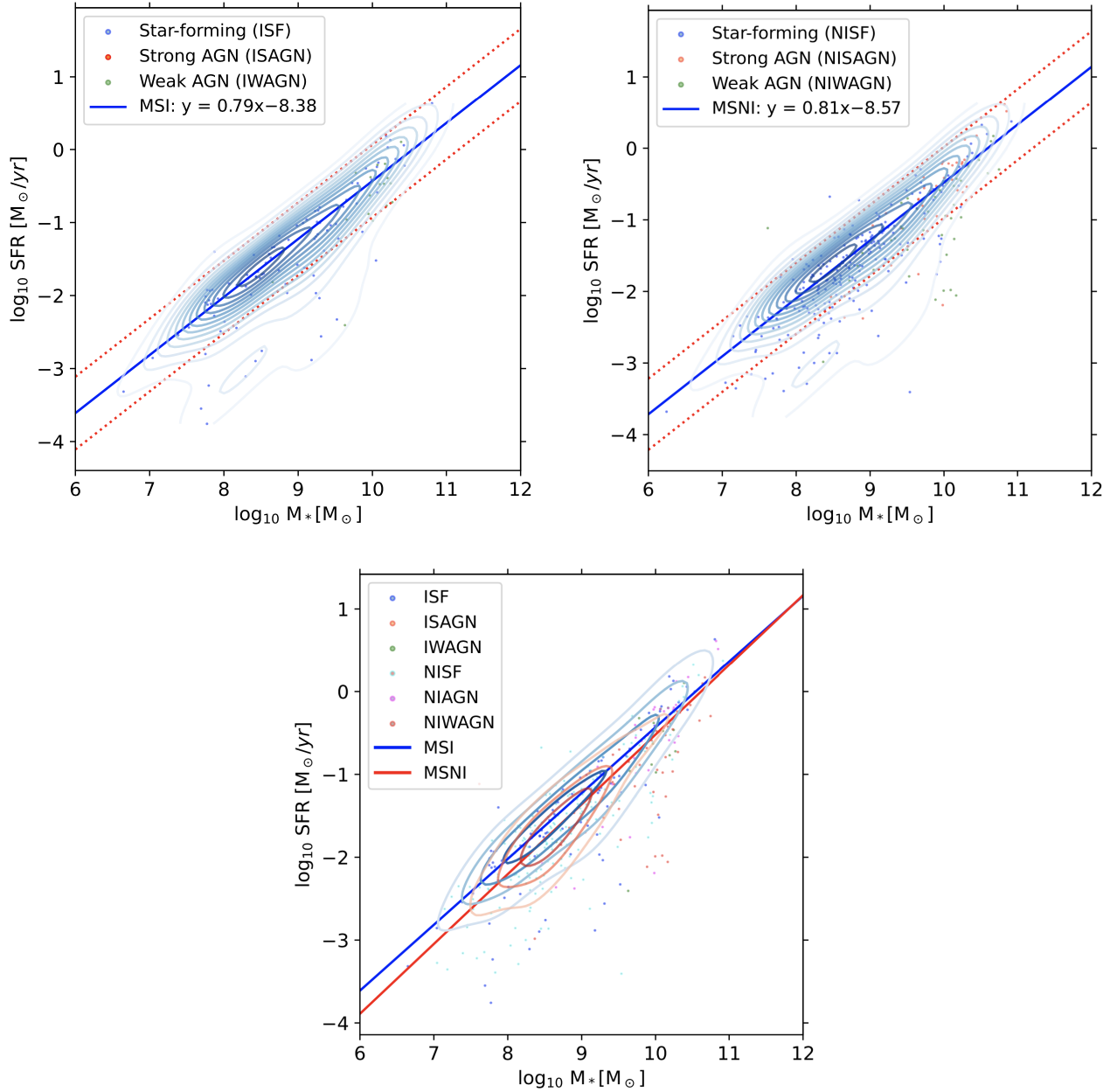


FIG. 5. Star formation main sequence for quenching galaxies: isolated sample (top left panel), non-isolated sample (top right panel), isolated and non-isolated on the same plot (bottom panel).

(column 4) ageing galaxies, respectively and SF (column 5), strong AGN (column 6), weak AGN (column 7) quenching galaxies, respectively. These tables are used to trace how the positioning of galaxies with respect to MS and GV are affected by changing the galaxies' environment and the influence of nuclear activity on the relation.

## V. DISCUSSION

From Fig. 1, it is observed that the number of star-forming galaxies decreases by  $\sim 12\%$  between isolated and non-isolated environments, while the retired galaxies increase by  $\sim 14\%$ , the number of strong AGN decreases by  $\sim 3\%$  and the weak AGN increase by  $\sim 1\%$ . This indicates that the star-forming and retired galaxies are more significantly affected by the environment than the AGNs, hence environmental dependence is influenced by the presence of AGN sources. From Fig. 2 it is observed that the ageing galaxies decrease by  $\sim 14\%$ , while the retired galaxies increase by  $\sim 14\%$ . The undetermined galaxies decrease by

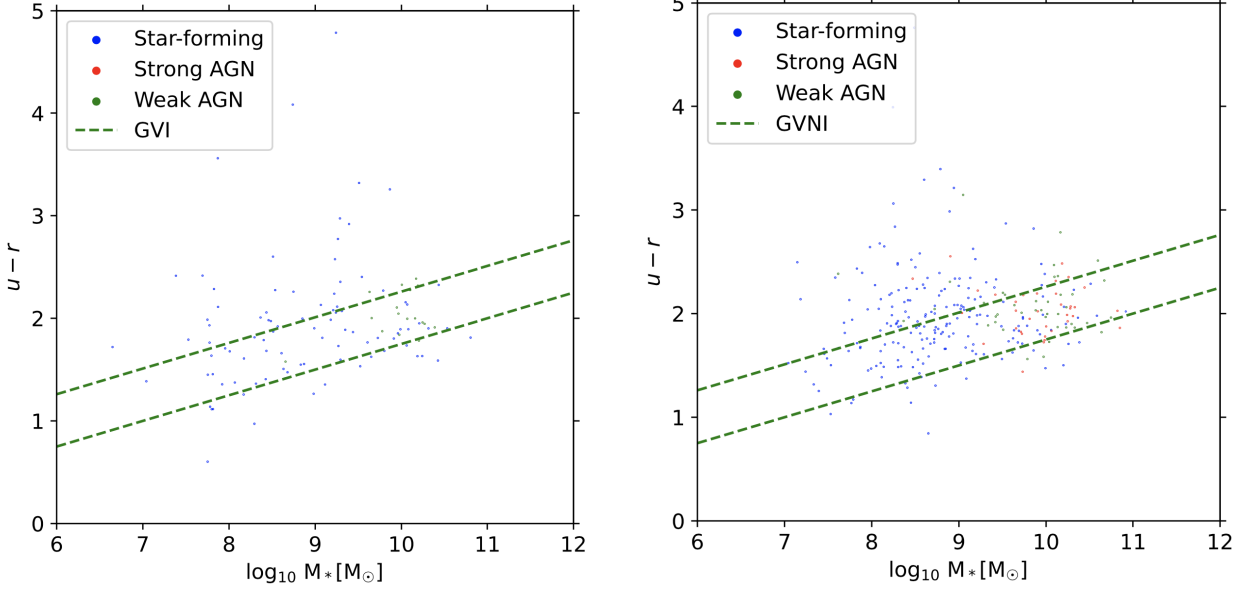


FIG. 6. Quenching galaxies'  $u - r$  colour against stellar mass diagrams for the isolated (left panel) and non-isolated (right panel) samples.

TABLE V. Chi-square P-values for ageing and quenching transitions between isolated and non-isolated galaxies within MS, above MS, and below MS.

Position (1)	Ageing			Quenching		
	Star-forming (2)	Strong AGN (3)	Weak AGN (4)	Star-forming (5)	Strong AGN (6)	Weak AGN (7)
MS	0.018	0.350	1	0.087	0.495	0.633
Above MS	0.001	0.942	0.656	0.251	0.730	0.072
Below MS	0.014	0.401	0.657	1	1	0.006

TABLE VI. Chi-square P-values for ageing and quenching transitions between isolated and non-isolated galaxies within GV, above GV, and below GV.

Position (1)	Ageing			Quenching		
	Star-forming (2)	Strong AGN (3)	Weak AGN (4)	Star-forming (5)	Strong AGN (6)	Weak AGN (7)
GV	0	0.113	0.139	0.943	0.763	0.928
Above GV	0.038	0.492	0.540	0.269	0.354	0.830
Below GV	0	0.055	0.063	0.269	0.108	0.310

$\sim 0.2\%$  while quenched galaxies increase by  $\sim 0.3\%$  between isolated and non-isolated environments. This proves the scenario of Fig. 1, where the ageing (which mostly contains star-forming galaxies, see Ref. [27]) and retired galaxies are strongly affected by the environment than undetermined and quenched galaxies. This trend shows that quenched and retired galaxies are found in non-isolated environments rather than isolated environments while ageing is primarily found in isolated rather than non-isolated environments. The study agrees with Ref. [28] using the density approach that quenched galaxies are primarily found in dense while ageing galaxies are found in less dense environments.

From Fig. 3 and Eqs. (10) and (11), the difference of  $\sim 0.03$  in slope and  $\sim 0.30$  in intercept are observed between isolated and non-isolated environment for ageing galaxies. The differences in slope and intercept are greater than the errors in slopes (0.01) and intercept (0.14). Furthermore, these differences produce P-values of  $5.190 \times 10^{-5}$ , and  $6.408 \times 10^{-5}$  for the slope and intercept, respectively which are both far less than the standard P-value in statistics (0.05). These two facts indicate that there is

a significant difference in slope and intercept between isolated and non-isolated environments for transition ageing galaxies.

From Fig. 5 and Eqs. (14) and (15), the difference of 0.02 in slope and 0.19 in intercept are observed between isolated and non-isolated environment for quenching galaxies. The difference in slope and intercept are less than the errors in slopes (0.06, 0.04) and intercepts (0.52, 0.34). Furthermore, these differences produce P-values of 0.50, and 0.36 for the slope and intercept, respectively which are both greater than the standard P-value in statistics (0.05). These two facts indicate that there is no significant difference in slope and intercept between isolated and non-isolated environments for quenching galaxies.

From Tables I, II, III, and IV it is observed that the number of SF, strong AGN, and weak AGN with respect to the MS have different fractions for the isolated and non-isolated environments in both ageing and quenching galaxies. In this observation the study agrees with the findings by Ref. [39], that galaxies classified as MS, quiescent and passive exhibit different fractions across different environments. On the other hand, the study agrees with Ref. [28], that ageing and quenching galaxies are found in different environments.

From column (2) of Table V, it is observed that the chi-square ( $\chi^2$ ) P-value for the difference in numbers of ageing galaxies between isolated and non-isolated within MS, above MS, and below MS is smaller ( $\sim 0.011$  on average) than the threshold (0.05) while from column (3) and (4) of Table V, it is observed that the P-values are greater ( $\sim 0.564, \sim 0.771$  on average) than the threshold (0.05). On the other hand from columns (5), (6), (7) of Table V, it is observed that the P-values are greater ( $\sim 0.446, \sim 0.742, \sim 0.237$  on average) than the threshold. Based on these observations, the positioning of SF ageing galaxies along the MS is affected by the environment, while the AGNs are not affected by the environment. The positioning of quenching galaxies is not influenced by the environment and this trend does not depend on the nature of nuclear activities of a particular galaxy.

From column (2) of Table VI, it is observed that the chi-square ( $\chi^2$ ) P-value for the difference in numbers of ageing galaxies between isolated and non-isolated within MS, above MS, and below MS is smaller ( $\sim 0.013$  on average) than the threshold (0.05) while from columns (3) and (4) of Table VI, it is observed that the P-values are greater ( $\sim 0.220, \sim 0.247$  on average) than the threshold. On the other hand from columns (5), (6), (7) of Table VI, it is observed that the P-values are greater ( $\sim 0.494, \sim 0.408, \sim 0.689$  on average) than the threshold. All these observations imply that the positioning of SF ageing galaxies with respect to the GV is affected by the environment, while the AGNs are not affected by the environment. The positioning of quenching galaxies with respect to the GV is not influenced by the environment and again this trend is not affected by the nature of nuclear activities of a particular galaxy.

## VI. SUMMARY AND CONCLUSION

This study aimed at investigating if the environment is among the factors affecting the slow decrease (ageing), and fast decrease (quenching) of SFR in galaxies and how the relationship is influenced by the nuclear activity of a particular galaxy at the transition stage. We used the friends-of-friends method (defined in Section III) to assign the volume-limited sample from SDSS DR 12 galaxies into isolated and non-isolated environments. From a flux-limited sample of SDSS DR12, we constructed the volume-limited sample of 136274 galaxies within  $-22.5 \leq M_r \leq -20.5$  (mag), containing 58032 ( $\sim 43\%$ ) isolated and 78233 ( $\sim 57\%$ ) non-isolated galaxies. The galaxies were classified according to their nature of nuclear activity employing WHAN diagnostic diagrams (shown by Fig. 1) into star-forming, strong AGN, weak AGN, and retired galaxies aiming to investigate the influence of nuclear activity on the environmental dependence of galaxies. Ageing diagrams (shown by Fig. 2) were used to classify the galaxies into ageing, quenched, undermined, and retired galaxies. Since we aim to study the ageing and quenching galaxies in the transition stage, we used the  $0.5 < (g - r) < 0.7$ , criteria from Ref. [27], to obtain a total number of 33452 ageing, galaxies in transition stage (AGT) where 16929 are isolated and 16523 are non-isolated. Furthermore, a total number of 419 quenching (QGT) was obtained, where 133 are isolated and 286 are non-isolated. The AGT and QGT were used throughout the study to investigate the star formation main sequence and the colour stellar mass diagram for ageing galaxies (shown by Figs. 3 and 4) and quenching galaxies (shown by Figs. 5 and 6). The following significant findings are revealed via this study:

- Ageing galaxies are mostly found in isolated rather than the non-isolated environment while quenching galaxies are found in non-isolated rather than the isolated environment.
- The significant change in slope and intercept of the equation of star formation main sequence by 0.03 dex, 0.30 dex respectively between isolated and non-isolated environments for ageing galaxies was observed indicating that the slope and intercept of ageing star formation main sequence are influenced by the environment.
- The insignificant change in slope and intercept of the equation of star formation main sequence by 0.02 dex, 0.12 dex respectively between isolated and non-isolated environments for quenching galaxies was observed indicating that the slope and intercept of quenching star formation main sequence are not influenced by the environment.
- A significant change in the number of ageing SF galaxies above, within and below the main sequence, similarly above, within and below the green valley between isolated and non-isolated environments was observed indicating that the po-

sitioning of ageing star forming galaxies with respect to the main sequence and the green valley is influenced by the environment. On the other hand insignificant change in the number of ageing strong and weak AGN was observed indicating that the positioning of ageing AGN are not influenced by the environment. This implies that ageing depends on the environment and this relationship is influenced the nuclear activity.

- An insignificant change in the number of quenching SF, strong AGN, and weak AGN was observed above, within and below the main sequence, similarly above, within and below the green valley between isolated and non-isolated environments was observed indicating that the positioning of quenching star forming galaxies with respect to the main sequence and the green valley are not influenced by the environment and the nuclear activity have negligible influence on the independence of quenching on the environment.

#### ACKNOWLEDGEMENTS

PP acknowledges support from The Government of Tanzania through the India Embassy, Mbeya University of Science and Technology (MUST) for Funding and SDSS for providing data. UDG is thankful to the Inter-University Centre for Astronomy and Astrophysics (IUCAA), Pune, India for the Visiting Associateship of the institute. Funding for SDSS-III has been provided by the Alfred P. Sloan Foundation, the Participating Institutions, the National Science Foundation, and the U.S. Department of Energy Office of Science. The SDSS-III website is <http://www.sdss3.org/>. SDSS-III is managed by the Astrophysical Research Consortium for the Participating Institutions of the SDSS-III Collaboration including the University of Arizona, the Brazilian Participation Group, Brookhaven National Laboratory, Carnegie Mellon University, the University of Florida, the French Participation Group, the German Participation Group, Harvard University, the Instituto de Astrofísica de Canarias, the Michigan State/Notre Dame/JINA Participation Group, Johns Hopkins University, Lawrence Berkeley National Laboratory, Max Planck Institute for Astrophysics, Max Planck Institute for Extraterrestrial Physics, New Mexico State University, New York University, Ohio State University, Pennsylvania State University, University of Portsmouth, Princeton University, the Spanish Participation Group, University of Tokyo, the University of Utah, Vanderbilt University, the University of Virginia, the University of Washington, and Yale University.

- 
- [1] G. Kauffmann, S. White, *The Environmental Dependence of the Relations between Stellar Mass, Structure, Star Formation and Nuclear Activity in Galaxies*, *MNRAS* **353**, 713 (2004) [[arXiv:astro-ph/0402030](#)].
- [2] C. Tremonti, T. Heckman, *The Origin of the Mass–Metallicity Relation: Insights from 53,000 Star-Forming Galaxies in the SDSS*, *ApJ* **613**, 898 (2004) [[arXiv:astro-ph/0405537](#)].
- [3] Y. Peng, S. Lilly, K. Kovač, M. Bolzonella, L. Pozzetti, A. Renzini, G. Zamorani, *Mass and Environment as Drivers of Galaxy Evolution in SDSS and zCOSMOS and the Origin of the Schechter Function*, *ApJ* **721**, 193 (2010) [[arXiv:1003.4747](#)].
- [4] J. Brinchmann, S. Charlot, *The physical properties of star forming galaxies in the low redshift universe*, *MNRAS* **351**, 1151 (2004) [[arXiv:astro-ph/0311060](#)].
- [5] D. Elbaz, E. Daddi, D. Borgne, *The reversal of the star formation-density relation in the distant universe*, *A&A* **468**, 33 (2007) [[arXiv:astro-ph/0703653](#)].
- [6] J. Speagle, C. Steinhardt, P. Capak, J. Silverman et al. *A Highly Consistent Framework for the Evolution of the Star-Forming “Main Sequence” from  $z \sim 0 - 6$* , *ApJS* **214**, 15 (2014) [[arXiv:1405.2041](#)].
- [7] S. Leslie, L. Kewley, D. Sanders, N. Lee *Quenching star formation: insights from the local main sequence*, *MNRAS* **455**, L82 (2015) [[arXiv:1509.03632](#)].
- [8] E. Daddi, M. Dickinson, G. Morrison, R. Chary et al. *Multiwavelength study of massive galaxies at  $z \sim 2$ . I. Star formation and galaxy growth*, *ApJ* **670**, 156 (2007). [[arXiv:0705.2831](#)].
- [9] T. Yuan, L. Kewley, D. Sanders, *The Role of Starburst-Active Galactic Nucleus Composites in Luminous Infrared Galaxy Mergers: Insights from the New Optical Classification Scheme*, *ApJ* **709**, 884 (2010)
- [10] J. Rich, L. Kewley, M. Dopita, *Galaxy-Wide Shocks in Late-Merger Stage Luminous Infrared Galaxies*, *ApJ* **782**, 9 (2014) [[arXiv:1104.1177](#)].
- [11] K. Schawinski, D. Thomas, M. Sarzi, C. Maraston et al. *Observational evidence for AGN feedback in early-type galaxies*, *MNRAS* **382**, 1415 (2007) [[arXiv:0709.3015](#)].
- [12] K. Whitaker, P. Dokkum, G. Brammer, M. Franx *The star formation mass sequence out to  $z = 2.5$* , *ApJL* **754**, L29 (2015) [[arXiv:1205.0547](#)].
- [13] T. Shimizu, R. Mushotzky, M. Meléndez, M. Koss et al. *Decreased specific star formation rates in AGN host galaxies*, *MNRAS* **452**, 1841 (2007) [[arXiv:1506.07039](#)].
- [14] T. Gonçalves, D. Martin, K. Menéndez-Delmestre, T. Wyder et al. *Quenching star formation at intermediate redshifts: downsizing of the mass flux density in the green valley*, *ApJ* **759**, 67 (2012) [[arXiv:1209.4084](#)].
- [15] J. Moustakas, A. Coil, J. Aird, M. Blanton, R. Cool et al. *Quenching star formation at intermediate redshifts: downsizing of the mass flux density in the green valley*, *ApJ* **767**, 50 (2013) [[arXiv:1301.1688](#)].

- [16] S. Faber, C. Willmer, C. Wolf, D. Koo, B. Weiner, J. Newman et al. *Galaxy Luminosity Functions to  $z \sim 1$ : DEEP2 vs. COMBO-17 and Implications for Red Galaxy Formation*, *ApJ* **665**, 265 (2007) [arXiv:astro-ph/0506044].
- [17] R. Hickox, J. Mullaney, D. Alexander, C. Chen, F. Civano et al. *Black hole variability and the star formation–active galactic nucleus connection: do all star-forming galaxies host an active galactic nucleus*, *ApJ* **782**, 9 (2014) [arXiv:1306.3218].
- [18] K. Schawinski, C. Urry, B. Simmons, L. Fortson, S. Kaviraj et al. *The green valley is a red herring: Galaxy Zoo reveals two evolutionary pathways towards quenching of star formation in early- and late-type galaxies*, *MNRAS* **440**, 889 (2014).
- [19] A. Fitts, M. Boylan-Kolchin, O. Elbert, J. Bullock et al. *fire in the field: simulating the threshold of galaxy formation*, *MNRAS* **471**, 3547 (2017).
- [20] J. Gensior, J. Kruijssen, B. Keller *Heart of darkness: the influence of galactic dynamics on quenching star formation in galaxy spheroids*, *MNRAS* **495**, 199 (2020).
- [21] L. Cortese, B. Catinella, R. Smith *The Dawes Review 9: The role of cold gas stripping on the star formation quenching of satellite galaxies*, *PASA* **38**, e035 (2021).
- [22] T. Brown, B. Catinella, L. Cortese, C. Lagos et al. *Cold gas stripping in satellite galaxies: from pairs to clusters*, *MNRAS* **466**, 1275 (2017).
- [23] M. Thorp, S. Ellison, H. Pan, L. Lin et al. *The ALMaQUEST Survey X: what powers merger induced star formation?*, *ApJ* **516**, 1462 (2022).
- [24] H. Akins, D. Narayanan, K. Whitaker, R. Davé et al. *Quenching and the UVJ Diagram in the SIMBA Cosmological Simulation*, *ApJ* **929**, 94 (2022).
- [25] S. Tacchella, C. Conroy, S. Faber, B. Johnson et al. *Fast, slow, early, late: quenching massive galaxies at  $z \sim 0.8$* , *ApJ* **926**, 134 (2022).
- [26] K. Suess, M. Kriek, R. Bezanson, J. Greene et al. *Studying Quenching in Intermediate- $z$  Galaxies—Gas, Momentum, and Evolution*, *ApJ* **926**, 86 (2022).
- [27] PabloCorcho-Caballero, Y. Ascasibar, S.F.Sanchez et al. *Ageing and quenching through the Ageing Diagram – II. Physical characterization of galaxies*, *MNRAS* **524**, 3692 (2023).
- [28] PabloCorcho-Caballero, Y. Ascasibar, S.F.Sanchez et al. *Ageing and quenching through the ageing diagram: predictions from simulations and observational constraints*, *MNRAS* **520**, 193 (2023).
- [29] F. Belfiore, R. Maiolino, K. Bundy, K. Masters et al. *SDSS IV MaNGA – sSFR profiles and the slow quenching of discs in green valley galaxies*, *MNRAS* **477**, 3014(2018).
- [30] N. Abdurro'uf, K. Accetta, C. Aerts, V. Silva et al. *The Seventeenth Data Release of the Sloan Digital Sky Surveys: Complete Release of MaNGA, MaStar, and APOGEE-2 Data*, *ApJ* **259**, 2 (2022).
- [31] G. Erfanianfar, P. Popesso, A. Finoguenov, D. Wilman et al. *Non-linearity and environmental dependence of the star-forming galaxies main sequence*, *MNRAS* **455**, 2839 (2016)[arXiv:1511.01899].
- [32] P. Lang, S. Wuyts, R. Somerville, N. Schreiber, R. Genzel et al. *Bulge Growth and Quenching since  $z = 2.5$  in CANDELS/3D-HST*, *ApJ* **788**, 788 (2014)[arXiv:1402.0866].
- [33] Bluck, Asa F. L., Maiolino, Roberto, Sánchez, Sebastian F., Ellison, Sara L. et al. *Are galactic star formation and quenching governed by local, global, or environmental phenomena?*, *MNRAS* **492**, 96 (2020).
- [34] J. Leja, Joshua S. Speagle, Y. Ting, Benjamin, D. Johnson et al. *A New Census of the  $0.2 < z < 3.0$  Universe. II. The Star-forming Sequence*, *ApJ* **936**, 165 (2022).
- [35] J. E Thorne, A. Robotham, L. Davies, S. Bellstedt, et al. *Deep Extragalactic Visible Legacy Survey (DEVILS): SED fitting in the D10-COSMOS field and the evolution of the stellar mass function and SFR– $M_*$  relation*, *MNRAS* **505**, 540 (2021).
- [36] S. Leslie, E. Schinnerer, D. Liu, B. Magnelli et al. *The VLA-COSMOS 3 GHz Large Project: Evolution of Specific Star Formation Rates out to  $z \sim 5$* , *ApJ* **899**, 58 (2020).
- [37] D. Croton, V. Springel, S. White, G. Lucia et al. *The many lives of active galactic nuclei: cooling flows, black holes and the luminosities and colours of galaxies*, *MNRAS* **365**, 11 (2013) [arXiv:astro-ph/0508046].
- [38] D. Rosario, P. Santini, D. Lutz, L. Shao et al. *The mean star formation rate of X-ray selected active galaxies and its evolution from  $z \sim 2.5$ : results from PEP-Herschel*, *A & A* **545**, A45 (2012) [arXiv:1203.6069].
- [39] A. Oemler, L. Abramson, M. Gladders, A. Dressler et al. *The Star Formation Histories of Disk Galaxies: The Live, the Dead, and the Undead*, *ApJ* **844**, 45 (2017).
- [40] SM. Croom, JS. Lawrence, J. Bland-Hawthorn, JJ. Bryant et al. *The Sydney-AAO multi-object integral field spectrograph*, *MNRAS* **421**, 872 (2012).
- [41] JJ. Bryant, MS. Owers, ASG. Robotham, SM. Croom et al. *The SAMI Galaxy Survey: instrument specification and target selection*, *MNRAS* **447**, 2857 (2005).
- [42] E. Tempel, T. Tuvikene, *Merging groups and clusters of galaxies from the SDSS data. The catalogue of groups and potentially merging systems*, *A & A* **602**, A100 (2017) [arXiv:1704.04477].
- [43] P. Ade, N. Aghanim, *Planck 2015 results. XXIII. The thermal Sunyaev-Zeldovich effect–cosmic infrared background correlation*, *A & A* **594**, A23 (2016) [arXiv:1509.06555].
- [44] D. Eisenstein, D. Weinberg, *SDSS-III: Massive spectroscopic surveys of the distant universe, the Milky Way, and extra-solar planetary systems*, *AJ* **142**, 72 (2011) [arXiv:1101.1529].
- [45] S. Alam, F. Albareti, C. Prieto, *The Eleventh and Twelfth Data Releases of the Sloan Digital Sky Survey: Final Data from SDSS-III*, *ApJS* **219**, 12 (2015) [arXiv:1501.00963].
- [46] David J. Schlegel, Douglas P. Finkbeiner, and Marc Davis. *Maps of dust infrared emission for use in estimation of reddening and cosmic microwave background radiation foregrounds*, *ApJ* **500**, 525 (1998).
- [47] Michael A. Strauss, David H. Weinberg, Robert H. Lupton, Vijay K. Narayanan et al. *Spectroscopic target selection in the Sloan Digital Sky Survey: the main galaxy sample*, *AJ* **124**, 3 (2002).

- [48] M. Blanton, S. Roweis, *K-corrections and filter transformations in the ultraviolet, optical, and near-infrared*, *AJ* **133**, 734 (2007) [arXiv:astro-ph/0606170].
- [49] M. Blanton, D. Hogg, N. Bahcall, J. Brinkmann et al *The galaxy luminosity function and luminosity density at redshift  $z = 0.1$* , *AJ* **592**, 819 (2003) [arXiv:astro-ph/0210215].
- [50] E. Tempel, E. Tago, L. Liivamägi *Groups and clusters of galaxies in the SDSS DR8-Value-added catalogues*, *A&A* **540**, A106 (2012) [arXiv:1112.4648].
- [51] E. Tempel, A. Tamm, M. Gramann, *Flux- and volume-limited groups/clusters for the SDSS galaxies: catalogues and mass estimation*, *A&A* **566**, A1 (2014) [arXiv:1402.1350].
- [52] N. M. Ball, J. Loveday, R. J. Brunner, I. K. Baldry, J. Brinkmann et al. *Bivariate galaxy luminosity functions in the Sloan Digital Sky Survey*, *MNRAS* **373**, 845 (2006).
- [53] P Schechter. *An analytic expression for the luminosity function for galaxies.*, *ApJ* **203**, 297 (1976).
- [54] X. Deng, Y. Xin, P. Wu, P Jiang et al. *Some Properties of Active Galactic Nuclei in the Volume-limited Main Galaxy Samples of SDSS DR8*, *ApJ* **754**, 82 (2012).
- [55] C. Kennicutt, *Star Formation in Galaxies Along the Hubble Sequence*, *A&A* **39**, 189 (1998) [arXiv:astro-ph/9807187].
- [56] S. Salim, J. Lee, R. Davé, *On the Mass-Metallicity-Star Formation Rate Relation for Galaxies at  $z \sim 2$* , *ApJ* **808**, 14pp (2015) [arXiv:1506.03080].
- [57] S.F. Sanchez, V. Avila-Reese, H. Hernandez-Toledo, E. Cortes-Suarez et al. *SSDSS IV MaNGA - Properties of AGN host galaxies*, *RxMAA* **54**, 1 (2018).
- [58] R. Cid Fernandes, G. Stasinska, A. Mateus and N. Vale Asari *A comprehensive classification of galaxies in the Sloan Digital Sky Survey: how to tell true from fake AGN*, *MNRAS* **413**, 1687 (2011).
- [59] L. Kewley, B. Groves, G. Kauffmann, T. Heckman et al. *The host galaxies and classification of active galactic nuclei*, *MNRAS* **372**, 961 (2006) [arXiv:astro-ph/0605681].
- [60] G. Kauffmann, T. Heckman, C. Tremonti, J. Brinĉhmann et al. *The host galaxies of active galactic nuclei*, *MNRAS* **346**, 1055 (2003) [arXiv:astro-ph/0304239].
- [61] L. Kewley, M. Dopita, R. Sutherland, C. Heisler et al. *Theoretical modeling of starburst galaxies*, *ApJ* **556**, 121 (2001) [arXiv:astro-ph/0106324].
- [62] R. Singh, G. van de Ven, K. Jahnke, M. Lyubenova et al. *The nature of LINER galaxies*, *A&A* **558**, A43 (2013)
- [63] Sebastián F. Sánchez *Spatially Resolved Spectroscopic Properties of Low-Redshift Star-Forming Galaxies*, *ARA&A* **99**, 58 (2020).
- [64] Sánchez, S. F., Walcher, C. J., Lopez-Cobá, C. Barrera-Ballesteros, J. K. *From Global to Spatially Resolved in Low-Redshift Galaxies*, *RxMAA* **57**, 3 (2021).